UDC 669.017:669-175.2+620.193

Structure and properties of 45 grade steel after equal-channel angular pressing at 400 °c

S.I. Pinchuk, G.I. Raab, D.G. Tishkevich, V.F. Balakin, V.V. Lysak

National Metallurgical Academy of Ukraine, Dnipropetrovsk, Ukraine

Abstract

The effect of severe plastic deformation (SPD) by equal-channel angular pressing on structure transformation and changes in the properties of 45 grade steel was studied. After four cycles of equal-channel angular pressing at 400°C, a significant refinement of the steel grain structure and improvement in its strength characteristics occur. Quantitative assessment of the change in parameters of the crystalline structure of ferrite and cementite as a result of severe plastic deformation was obtained. The influence of the structure formed by SPD on the steel corrosion behavior was defined.

Keywords: *severe plastic deformation, equal-channel angular pressing, structure, subgrain, properties, corrosion rate.*

Introduction

In the processes of production and transportation of oil and gas, tubes are exposed to a combined effect of significant mechanical loads and attack of corrosive media. It results in frequent mechanical and corrosion damaging of tubes followed by their premature failures. Use of carbon steel grades and conventional rolling processes does not ensure sufficient reliability of oil and gas pipe operation despite application of corrosion protection measures. The necessary improvement of service properties of oil and gas pipes requires formation of a more perfect metal structure, strength properties and corrosion behavior through an application of not only conventional but up-to-date rolling processes.

Physical-mechanical properties and corrosion behavior of steels much depend on a degree of granulation and homogeneity of metal structure. Application of severe plastic deformation (SPD) can be effective for fine-grain structure formation [1-5]. SPD ensures alteration of the dislocation structure in metal and allows obtaining metal products with a pore-free homogeneous, nano- and submicrocrystalline material structures in which large-angle grain boundaries prevail in a nonequilibrium state [6, 7]. Such structure transformation secures a significant improvement of strength properties and satisfactory plasticity of metals.

At the same time, improvement in strength characteristics can be accompanied by improvement of metal corrosion behavior [8, 9]. However the available information on the effect of SPD on corrosion behavior of metals is varied. For example, works [10, 11] did not mention

changes in corrosion behavior of nickel and copper during SPD. Work [12] observed decrease in corrosion resistance. According to the data obtained in [13], SPD promotes increase in metal resistance to pitting corrosion which manifests itself in higher values of pitting potential and density of corrosion current in electrically conducting media. The pitting mechanism can be associated with formation of local microscopic galvanic cells between the metallic matrix (anode) and Si-containing admixtures (cathode) in the metal surface after SPD. With the growth of SPD cycle number, admixture particles get smaller and their more even distribution in metals occurs resulting in a reduction of cathode area and growth of pitting corrosion resistance. Enhanced resistance of nano- and submicrocrystalline materials to pitting corrosion can be also explained by a rapid formation of a relatively dense film on the surface of crystal defects [14, 15]. The film with a large number of grain boundaries, a considerable share of nonequilibrium grain boundaries and residual stresses can be relatively stable in Cl-containing media [16]. At the same time, the higher density of grain boundaries in such materials can speed up corrosion because of a higher density of active centers of anodic dissolution under the influence of a corrosive medium.

This paper presents information on the effect of SPDB upon structure, strength properties and corrosion behavior of carbon steels used in making tubes for the production and transportation of oil and gas.

Material and procedures

Properties of commercial 45 grade steel with ferrite-pearlite structure were studied before and after SPD using equal-channel angular pressing (ECAP). Steel samples were subjected to ECAP at 400 °C by their extrusion through a die with channels crossing at an angle of 120°. SPD experiments included 4 pressing cycles with turning of the steel sample by 90° round the longitudinal axis after each cycle.

Microstructure was investigated by light microscopy and the structure images were analyzed by means of Structure 2001 software package. Fine structure of the steel was studied by means of JEM-2000SX-II electron microscope at accelerating voltage 200 kV. Rigaku Ultima IV diffractometer was used for X-ray structure analysis with CuK_{α} emission.

Corrosion behavior of steel samples before and after SPD was assessed by gravimetric method using the test data obtained in G-4 climate cell at air temperature 40 °C and humidity up to 98% and by potentiostatic method using PI-50-1 potentiostat. Optical microscope Neophot 2 and scanning electron microscope SEM-106-I were used in analysis of the sample surface condition after corrosion tests.

Study findings

As it was established in the studies, the samples of 45 grade steel in their initial state had a ferrite-pearlite structure with an average ferrite grain size of 40 to 60 μm (Fig. 1, *a*). Density of dislocations in redundant ferrite and ferrite component in perlite was not higher than 5×10^{8} cm^{-2}. Pearlite component features a plate structure with a distance about 0.1 to 0.3 μm between the plates.

Fine structure study has revealed multiple ruptures in pearlite plates which are structure defects in the cementite skeleton of colonies (Fig. 1, *b*). These ruptures are connected with the fact that a series of morphological transformations (from plates to bands or rods) in pearlite occur in the course of development of the cementite component [17]. Diffraction patterns show that both ferrite and cementite reflections are of a centrally symmetrical shape with no azimuthal blur which indicates on the absence of considerable dislocation aggregates and dislocation walls (Fig. 1, *c*). Interpretation of electron-diffraction patterns (Fig. 1, *d*) shows that Isaichev orientation and dimensional conformity [18] takes place which differs from Bagariatsky orientation conformity (OC) [19] by angle 3.5°. Pitch orientation conformance [20] was also observed.

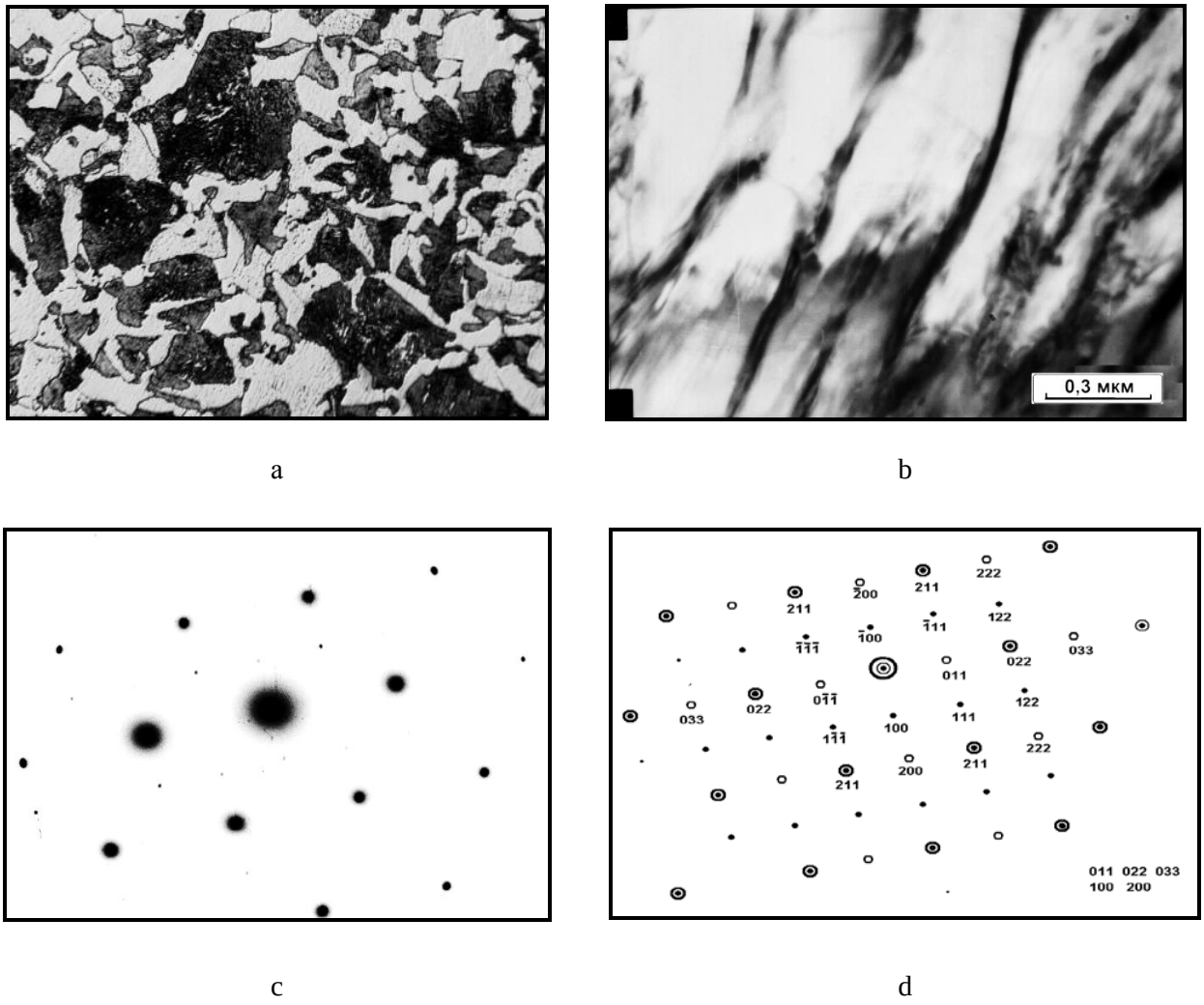

a b c d

Fig.1 Microstructure and crystallography in 45 grade steel samples in initial state: ferrite-pearlite structure (*a*); fine perlite structure (*b*); electron-diffraction pattern from the chosen ∅ 3 μm area (*c*); scheme of interpretation of an electron-diffraction pattern with orientation $(111)_\alpha \parallel (011)_\theta$ in accordance with Pitch orientation conformance between ferrite and cementite lattices (*d*)

A pronounced cellular substructure with an average fragment size of 500 to 800 μm was observed in steel subjected to ECAP (Fig. 2, *a*). As SPD temperature was equal to 400 °C, polygonization took place in the postdeformation period. Internal volumes of polygons (subgrains) got free from dislocations to a considerable degree. After SPD, ferrite and cementite plates in the pearlite component were bent and saturated with defects (Fig. 2, *b*) and numerous polygonal walls consisted of uniform grids of redundant dislocations (Fig. 2, *c*) which remained noncompensated after annihilation of opposite-sign dislocations.

Dislocation density ρ was approximately equal to $9 \cdot 10^{10}$ cm^{-2}.

Strands between reflections in $[001]_ц$ directions were observed in diffraction patterns which is an indication of existence of stacking faults of a deformation origin in the plates of θ-phase (Fig. 2, *d*).

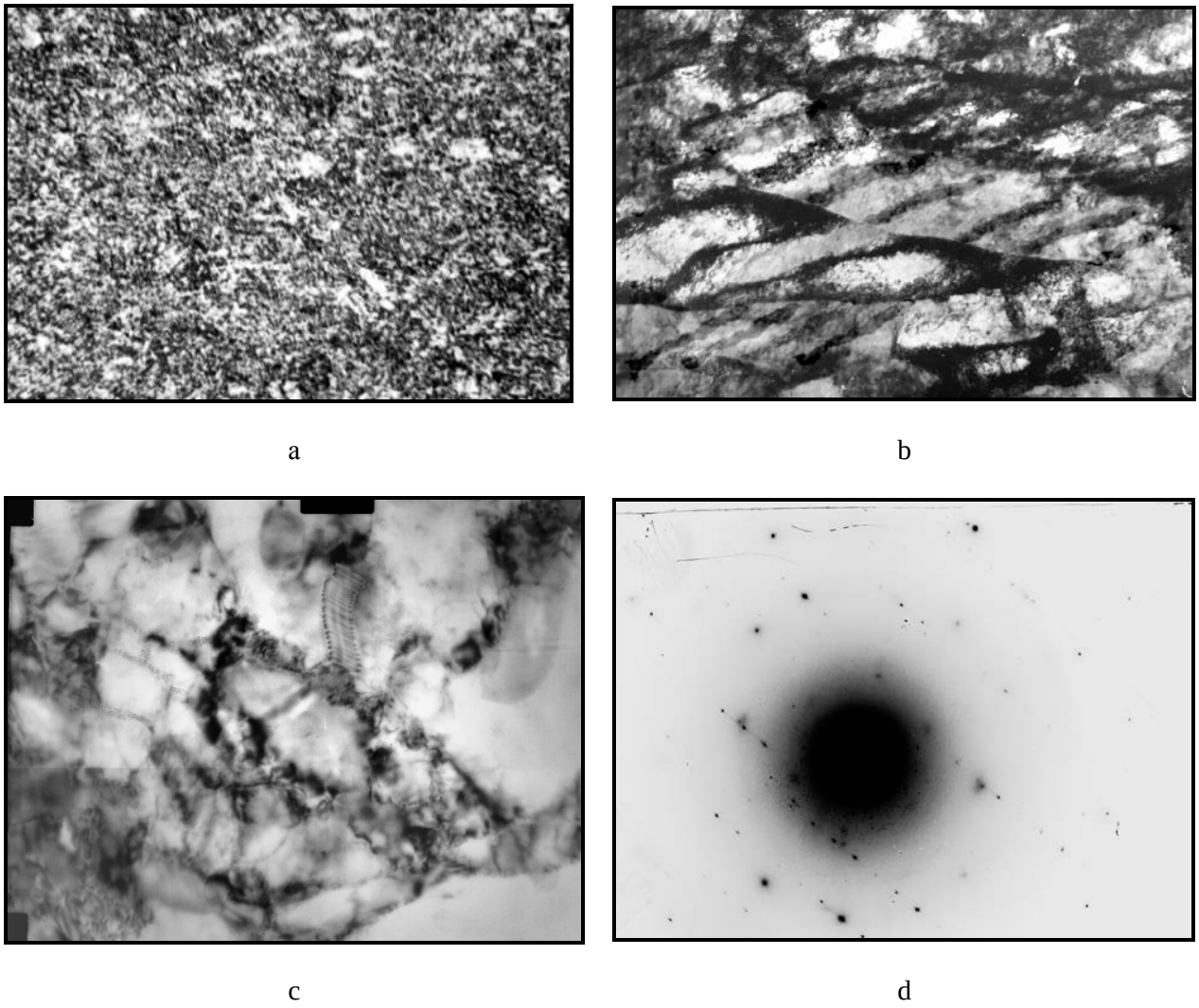

a b c d

Fig. 2 Structure and crystallography of 45 grade steel samples after ECAP: microstructure, ×1,000 (*a*); ferrite-cementite mixture, ×74,000 (*b*); fine-grain ferrite structure, ×50 000 (*c*); diffraction pattern with reflections elongated in $[001]_{ц}$ direction (*d*)

Elastic deformation of separate blocks and crystals in the process of ECAP promoted decrease in microdeformations of ferrite and cementite lattices (Table 1). Parameter of the ferrite lattice did not change.

Table 1 Parameters of ferrite and cementite lattices before and after ECAP

Structure state	Parameters				
	a, nm	b, nm	c, nm	Volume of crystal lattice V, nm^3	Microdeformation $\Delta a/a \times 10^{-3}$
Ferrite					
Initial	0.2868	-	-	0.02359	3.6
After deformation	0.2868	-	-	0.02359	3.0
Cementite					
Initial	0,4900	0.6670	0,4454	0.1450	2.3
After deformation	0.5040	0.6130	0.4770	0.1470	2.1

Transformation of steel structure resulted from dislocation rearrangement during ECAP enhances strength properties of steel. Ultimate strength increases from 600 to 875 MPa, yield strength from 330 to 605 MPa, hardness from171 to 250 HV.

Study of corrosion behavior of steel samples before and after ECAP has shown that centers of attack in conditions of humid air formed within a drop of liquid condensing in the metal surface. They developed as far as iron oxides appeared at the periphery of drop-shaped electrolyte zones. In the course of time, centers of attack increased their size and some of them contacted with each other forming more complex and larger complexes. The most active process of corrosion failure were obderved at the ferrite grain boundaries. Pearlite colonies were exposed to corrosion damage first. It is indicated by considerable accumulation of oxide material at the locations of pearlite colonies. It is because these colonies possess redundant energy due to a large quantity of ferrite-cementite interfaces in a volume unit of eutectoid colonies.

Extensive areas of corrosion attack were observed on the surface of 45 grade steel samples both before and after ECAP (Fig. 3).

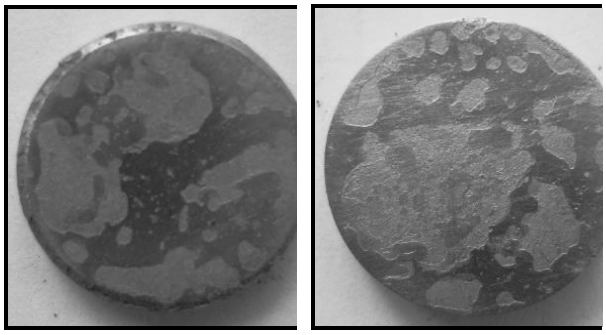

a b

Fig. 3 Surface of 45 grade steel samples in initial state (*a*) and after deformation by ECAP (*b*) after removal of corrosion products

As it is seen in Fig. 4, a considerable number of corrosion stains and local corrosion damages (dimples and pits) are present in the sample surface.

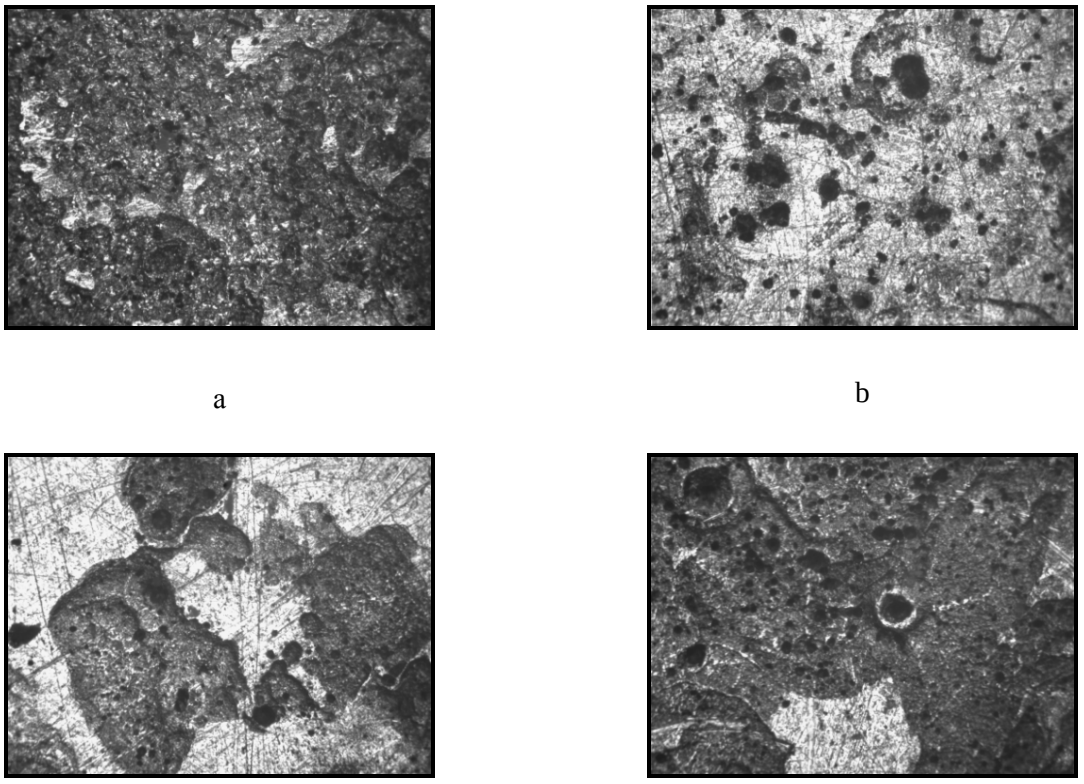

a b c d

Fig. 4 Pictures of various areas in the surface of 45 grade steel samples after accelerated atmospheric corrosion tests

in their initial state (*a*, *b*) and after deformation by ECAP (*c*, *d*)

According to the values of negative mass index K_m^- given in Fig. 5, average corrosion rates in steel samples were practically equal before and after deformation (Fig. 5, *a*). However according to the dynamics of change of positive corrosion rate index K_m^+ (Fig. 5, *b*) which characterizes mass increase resulting from the corrosion processes in the course of tests, it is evident that corrosion after ECAP was slower within first 40-50 hours of test in comparison with the samples in initial state.

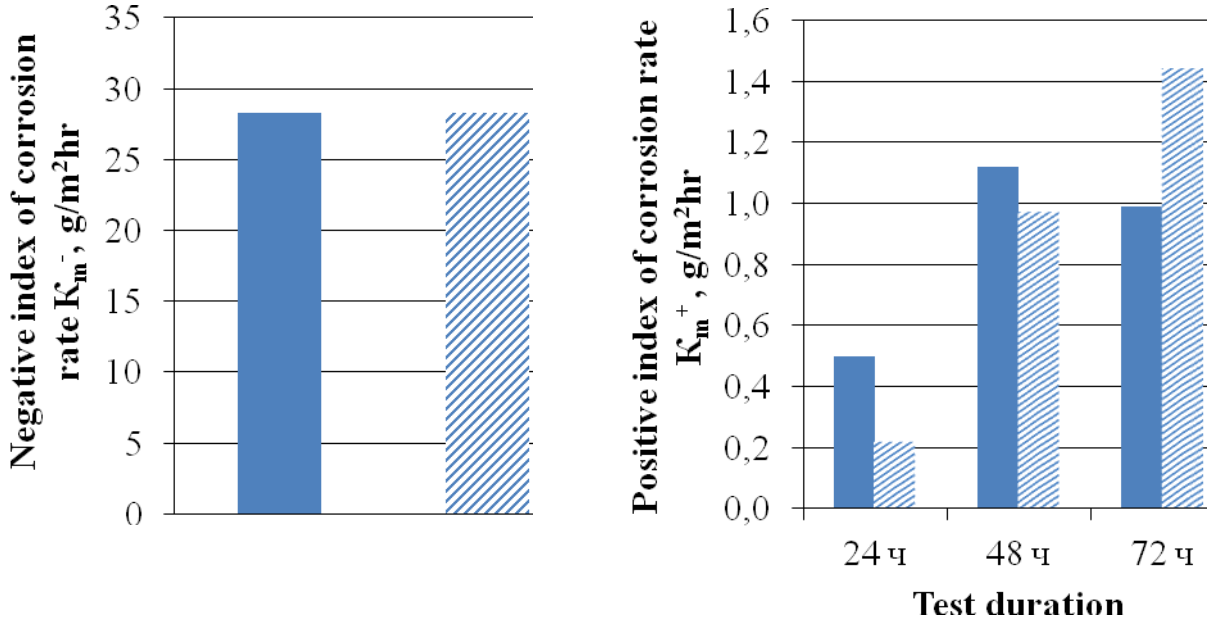

a b

Fig. 5 Average values of negative K_m^- (*a*) and positive K_m^+ (*b*) indices of corrosion rate in steel samples in initial ( ) and deformed ( ) states

According to the results obtained in electrochemical tests, rate of dissolution of deformed 45 grade steel samples is lower in a broad potential range as compared to that of the samples in their initial state (Fig. 6). Standard electrode potential of deformed 45 grade steel samples shifts in a positive direction which is an evidence of a higher resistance to electrochemical corrosion.

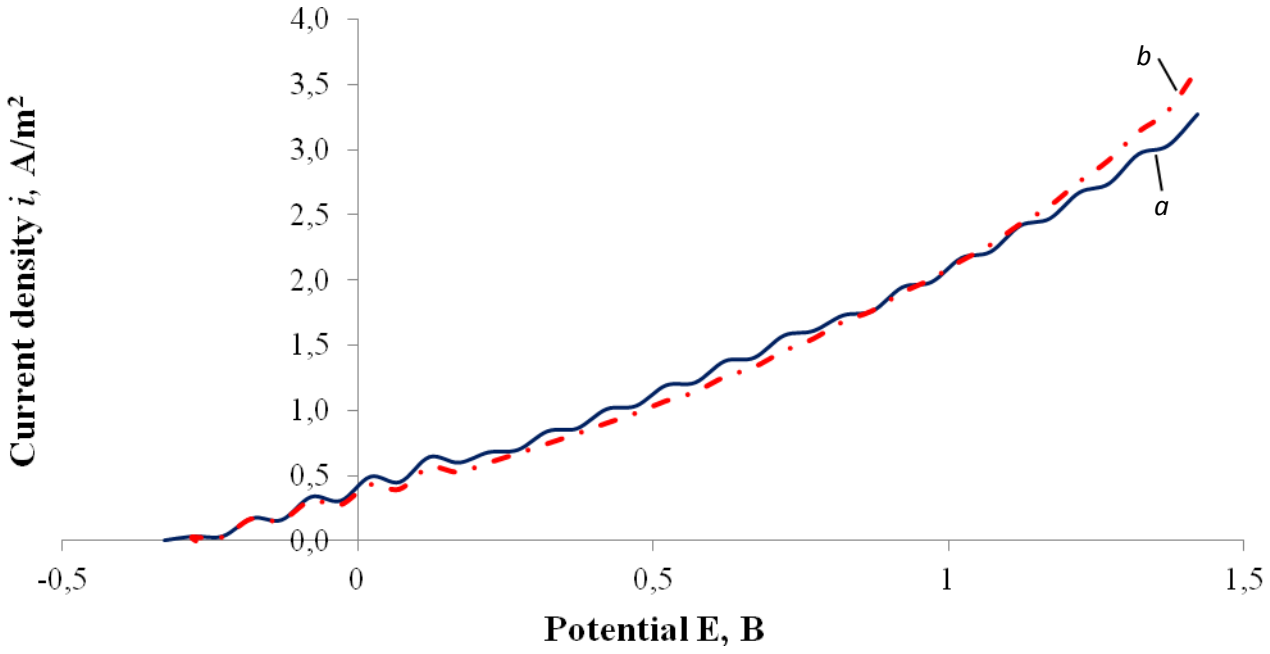

Fig. 6 Anode polarization curves characterizing corrosion of 45 grade steel samples before (*a*) and after (*b*) ECAP

Corresponding corrosion damage was observed in the sample surface. Quantity and sizes of these damages witness a more active dissolution of surface of 45 grade steel samples in their initial state (Fig. 7).

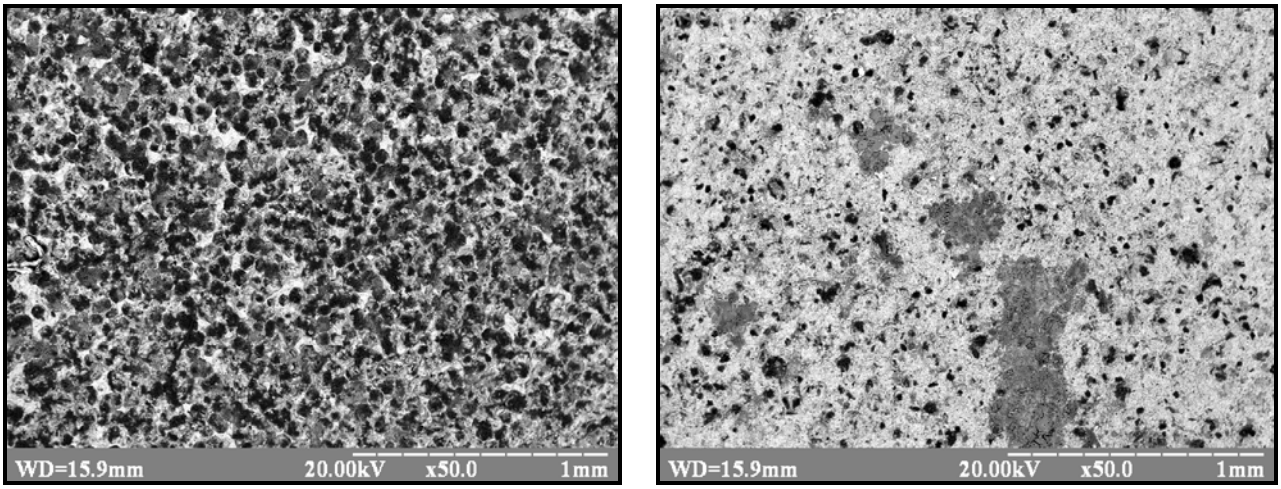

а б

Fig. 7 Surface of steel samples in initial state (a) and deformed state (b) after electrochemical tests

Measuring of corrosion damage depth after a 3-hour atmospheric corrosion tests has shown that the depth of damage penetration in deformed samples was smaller than in the samples in their initial state. It is in a complete conformance with abovementioned data of corrosion studies by gravimetric and electrochemical methods.

Conclusions

Equal-channel angular pressing (ECAP) of 45 grade steel results in transformation and

rearrangement of its dislocation structure and formation of a pronounced cellular substructure with an average cell size in a submicrocrystalline range.

Increase in dislocation density and formation of a developed subgrain structure in ECAP determine enhancement of strength properties of 45 grade steel. Growth of ultimate strength from 600 to 875 MPa, yield strength from 330 to 605 MPa and hardness from 171 to 250 HV was observed as well.

Study of corrosion behavior of steel samples after their ECAP has shown that the average corrosion rate in conditions of damp atmosphere remains at the level of initial samples. For the first 40-50 hours of testing, corrosion rate in samples after ECAP was lower as compared with the initial samples.

According to the results obtained in electrochemical tests, sample dissolution rate after ECAP was lower in a wide potential range as compared with that for the samples in their initial state. Standard electrode potential of deformed samples of 45 grade steel shifted in a positive direction which witnesses their higher resistance to electrochemical corrosion.

References

1. Valiyev R.Z. Obtainment of unique mechanical properties of 45 grade steel by severe plastic deformation / R.Z. Valiyev, N.G. Zaripov, M.V. Karavayeva, S.K. Nuriyeva // Nauchniye vedomosti Belgorodskogo gosudarstvennogo universiteta. Series: Mathematics. Physics, 2011. – Vol. 23. – No. 11. – p. 129-133.

2. Astafurova Ye.G. Microstructure features and mechanical behavior of 06MBF steel after equal-channel angular pressing / Ye.G. Astafurova, G.G. Zakharova, Ye.V. Naydenkov, G.I. Raab, P.D. Odessky, S.B. Dobatkin // Letters on materials, 2011. – Vol. 1. – s. 198-202.

3. Astafurova Ye.G. Effect of equal-channel angular pressing on structure and mechanical properties of low-alloy steel 10G2FT / Ye.G. Astafurrova, G.G. Zakharova, Ye.V. Naydenkin, S.V. Dobatkin, G.I. Raab // Fizika metallov I metallovedeniye. – 2010. – Vol. 110. – No. 3. – p. 275-284.

4. Shagalinaa S.V. Obtainment of a submicrocrystalline structure in steels St. 10 and 08P at equal-channel angular pressing / S.V. Shagalina, Ye.G. Korolyova, G.I. Raab, M.V. Bobyliov, S.V. Dobatkin // Metally. – 2008. – No. 3. – p. 44-51.

5. Yakovleva S.P. Integrated study of mechanical properties of low-alloy steel with a ultra-fine grain (200-600 nm) structure / S.P. Yakovleva, S.N. Makharova, M.Z. Borisova // Zavodskaya Laboratoriya. Diagnostika Materialov. – 2008. – Vol.74. – No. 1. – p.50-53.

6. Valiyev R. Z. Nanostructural materials obtained by severe plastic deformation / R. Z. Valiyev, I. B. Aleksandrov – M.: Logos, 2000. – 272 p.

7. Chuvildeyev V.N. Non-equilibrium grain boundaries in metals. Theory and applications / V.N. Chuvildeyev – M.: Fizmatizdat Publishers, 2004. – 304 p.

8. Chuvildeyev V.N. Effect of simultaneous increase of strength and corrosion resistance of microcrystalline titanium alloys / V.N. Chuvildeyev, V.I. Kopylov, A.M. Bakhmetyev, N.G. Sandler, A.V. Nokhrin et al. // Doklady Akademii Nauk. – 2012. – Vol. 442. – No. 3. – p. 329.

9. Khaydarov R.R. Corrosion resistance of aluminum alloys of 1421 and 5083 grades with ultra-fine grain structure subjected to electrochemical treatment in comparison with their coarse-grained analogues / R.R. Khaydarov // Bashkirsky Chimichesky Zhurnal – 2010. – Vol. 17. – No. 4. – p. 140-142.

10. Rofagha R. The corrosion behavior of nanocrystalline nickel / R. Rofagha, R. Langer, A. M. El-Sherik, U. Erb, G. Palumbo, K. T. Aust // Scripta Metallurgica. – 1991. – Vol. 25. – C. 2867-2872.

11. Vinogradov A. On the corrosion behavior of ultra-fine grain copper / A. Vinogradov, T. Mimaki, S. Hashimoto, R. Valiev // Scripta Materialia. – 1999. – Vol. 41. – C. 319-326.

12. Rofaga R. The effects of grain size and phosphorus on the corrosion of nanocrystalline Ni-P alloys / R. Rofaga, U. Erb, D. Ostander, G. Palumbo, K. T. Aust // Nanostructured Materials – 1993. – Vol. 2. – C. 1-10.

13. Chung M. Effect of the number of ECAP pass time on the electrochemical properties of 1050 Al alloys / M. Chung, Y. Choi, J. Kim, Y. Kim, J. Lee // Materials Science and Engineering A. – 2004. – V. 366. – P. 282-291.

14. Balyanov A. Corrosion resistance of ultra fine-grained Ti / A. Balyanov, J. Kutnyakova, N.A. Amirkhanova, V.V. Stolyarov, R.Z. Valiev, X.Z. Liao, Y.H. Zhao, Y.B. Jiang, H.F. Xu, T.C. Lowe, Y.T. Zhu // Scripta Materialia. – 2004. – V. 51. – P. 225-229.

15. Song D. Corrosion behavior of ultra-fine grained industrial pure Al fabricated by ECAP / D. Song, A. Ma, J. Jiang, P. Lin, D. Yang // Transactions of Nonferrous Metals Society of China. – 2009. – V. 19. – P. 1065-1070.
16. Qin L. Effect of grain size on corrosion behavior of electrodeposited bulk nanocrystalline Ni / L. Qin, J. Lian, Q. Jiang // Transactions of Nonferrous Metals Society of China. – 2010. – V. 20. – P. 82-89.
Sukhomlin G.D. Crystal geometry features of pearlite in hypoeutectoid steel // FMM. – 1976. – Vol. 42, Issue 5. – p. 965-970.
Isaichev I. V. Cementite orientation in tempered carbon steel // Zhurnal Tekhnicheskoy Fiziki – 1947, – Vol. 17. – p. 835-838.
Bagariatsky S.A. Probable mechanism of martensitedisintegration // Doklady Akademii Nauk SSSR – 1950, – Vol. 73. No. 6. – p. 1161-1164.
Pitsch W. Der Orientirungszusammenhang zwischen Zementit und Ferrit im Pearlit. // Acta Met. – 1962, – Vol. 10. – P. 79-80 (errata, “Acta Met.”, – 1962, – Vol. 10, – P. 906).